
Technical Report: Aggregation on Learnable Manifolds for Asynchronous Federated Optimization

Archie Licudi

Department of Engineering Science, Oxford University

archie.licudi20@alumni.imperial.ac.uk

Abstract

In Federated Learning (FL), a primary challenge to the server-side aggregation of client models is device heterogeneity in both loss landscape geometry and computational capacity. This issue can be particularly pronounced in clinical contexts where variations in data distribution (aggravated by class imbalance), infrastructure requirements, and sample sizes are common. We propose ASYNCMANIFOLD, a novel asynchronous FL framework to address these issues by taking advantage of underlying solution space geometry at each of the local training, delay-correction, and aggregation stages. Our proposal is accompanied by a convergence proof in a general form and, motivated through exploratory studies of local behaviour, a proof-of-concept algorithm which performs aggregation along *non-linear mode connections* and hence avoids barriers to convergence that techniques based on linear interpolation will encounter.

1 Introduction

In recent years, Federated Learning (FL) has seen a wave of research interest (Zhang et al., 2021; Xu et al., 2023) for its ability to keep data in private silos and achieve collaborative model training without the divulgence of centralised data. This has been particularly notable in the healthcare sector (Rieke et al., 2020; Soltan et al., 2023; Molaei et al., 2024), where balancing evolving legislation around the privacy of sensitive data and the performance of models with high-stakes outcomes is a priority. However, it faces a significant hurdle in the form of *client heterogeneity*, where the datasets on each client can differ in both size and underlying distribution (Ye et al., 2023); in the traditional distributed optimisation setting, this can be mitigated by pooling and re-allocating the data assigned to each client, an option not available to federated approaches. A particular form of client heterogeneity that arises in the healthcare setting is *computational imbalance* (Pfeiffer et al., 2023), where clients may differ in compute capacity along with dataset size, leading to some clients spending far longer to perform each optimisation step than others. A natural response to account for these “stragglers” is to allow for asynchronous updates (Xie et al., 2020), where clients are able to submit their results and receive an updated global model to continue training immediately, rather than waiting for all stragglers to submit to begin the next round.

Most FL systems in use today derive in some way from FEDAVG (McMahan et al., 2023), which at each communication round simply computes the new global model as the arithmetic mean of the local models. Due to the inherently irregular and non-convex nature of neural network loss landscapes (Li et al., 2018), however, this often fails to account for any degree of meaningful client heterogeneity as it rests on the assumption that linear interpolation between single-task models yields a multi-task model with comparable performance. In geometric terms, the underlying assumption of FEDAVG is that local minima of client losses form a convex polytope of low global loss in parameter space - a hypothesis which, especially as the models approach convergence, can often be poorly supported in practice (Zhou et al., 2023). In this paper, we present a novel framework for addressing this issue, unifying recent work on Riemannian optimisation (Nickel & Kiela, 2018; Bonnabel, 2013; An et al., 2023) with emerging empirical studies on the power of simple, non-linear “mode-connecting” curves (Garipov et al., 2018; Lubana et al., 2023) that allows for this polytope assumption to be relaxed to the existence of an arbitrary low-loss manifold, which can be specified *a priori* or learned during the optimisation process. Whilst our analysis is restricted to the class of SGD-

like local optimisers which take steps based on unbiased estimates of loss function derivative, we provide a convergence result that is agnostic of the manifold w.r.t. which the derivative is taken (under certain regularity assumptions), generalising Riemannian SGD to the federated setting. We provide a convergence proof for this family of algorithms in the asynchronous regime, from which synchronous convergence of the approach is a corollary.

Although asynchronicity maximises client utilisation, it encounters the problem of *delayed update*: the updates proposed by each client w.r.t. a previous version of the global model may no longer be appropriate by the time the update is received (Leconte et al., 2024). To mitigate this, we propose the ORTHOCORRECT method of delay correction which considers only the component of client update orthogonal to the global drift. We perform an analysis of the local (step-wise) efficacy of various approaches in the literature, uncovering the time-dependent nature of their performance, and demonstrating the superiority of orthogonal correction. We similarly explore the use of quadratic Bezier curves as a simple instance of a learnable manifold in our framework and show that, even where the control points are learned w.r.t. outdated global modes without delay correction, the curve exhibits lower average loss than the corresponding linear connection, justifying the use of learnable parameters within ASYNCMANIFOLD. To run these experiments, we developed an asynchronous fork of the Flower FL library (Beutel et al., 2022) in which each proposal was implemented.

Finally, guided by these explorations and requirements of mitigating heterogeneity arising in the healthcare setting, propose the ASYNCCURVE algorithm as a simple instantiation of our framework, which is parallelisable to run with no increase in wall-clock time in comparison to FEDAVG.

1.1 Related Work

Asynchronous FL McMahan et al. (2023) proposed the synchronous federated paradigm with simple geometric mean aggregation. Many proposals since have focused on mitigating the inconsistency between client datasets and hence model updates. Li et al. (2020) is a notable example, which adds a *proximal* L^2 regularisation term to the client losses, with Acar et al. (2021) implementing the same principle with a different regulariser. These ideas were adapted to the asynchronous setting in Xie et al. (2020). Karimireddy et al. (2021) is another synchronous approach to mitigating heterogeneity that can be intuitively asynchronised. Reddi et al. (2021) provides a framework for using adaptive aggregation on the server-side, the SGDm version of which has been adapted with delay-correction to the asynchronous setting in Shi et al. (2025); Wang et al. (2020b) is a proposal that seeks to mitigate heterogeneity where the *local* solvers are adaptive gradient optimisers. An interesting approach with ties to mode connectivity (Tatro et al., 2020) is Wang et al. (2020a), which aligns networks before aggregation according to the permutation equivariance of layers; although we do not adopt this in our proposal as we found the number of epochs which each client trains for in the standard federated setting rarely leads to misaligned models.

Mode Connectivity refers to the notion that different local minima (*modes*), even of models that are trained entirely independently, are often connected by simple curves of low average loss in parameter space, revealing a large, highly-connected subspace of good solutions (Garipov et al., 2018; Lubana et al., 2023). These studies focus on polynomial curves and polygon chains, with work such as Benton et al. (2021) extending these ideas to simplicial complexes; Grinwald et al. (2025) leverages a similar principle in the federated setting. An important implication of mode connectivity is its relation to the *flatness* of minima, conjectured to be correlated with a model’s generalisation ability (Haddouche et al., 2025), which has been examined in work such as (Izmailov et al., 2019; Guo et al., 2022). Zhou et al. (2023) shows a similar connection between the heterogeneity of multi-task losses and the existence of high-loss “barriers” along the linear connection, which may be alleviated by using polynomial connections. Work such as Sun et al. (2024) and Caldarola et al. (2022) more directly considers flatness-aware methods in the federated setting.

Riemannian Methods While mode connectivity is set on manifolds implicitly, there has been interest in the direct applications of Riemannian geometry to deep learning, with notable early work in Bonnabel (2013). The particular applications to hyperbolic space of Nickel & Kiela (2018) have also inspired work such as An et al. (2023) which compute proximal terms via the Riemannian metric of a space which is projected onto.

2 Background and Preliminaries

2.1 Notation

We use $[n]$ for $n \in \mathbb{N}$ to denote the set $\{1, 2, \dots, n-1, n\}$ of natural numbers ≥ 1 but $\leq n$; similarly $[n..m]$ for $n, m \in \mathbb{Z}$ denotes the set $\{n, n+1, \dots, m-1, m\}$ of integers $\geq n$ but $\leq m$. Matrix-matrix and matrix-vector multiplication is denoted by concatenating the symbols, e.g. M_1M_2 and Mv respectively. The entry-wise (Hadamard) product is denoted \odot .

2.2 Problem Setting

We consider Asynchronous Federated Minimisation over N clients. Formally, we are interested in solving optimisation problems of the form:

$$\min_{\theta \in \mathbb{R}^\Theta} \mathcal{L}(\theta) := \frac{1}{N} \sum_{i=1}^N \mathcal{L}_i(\theta) \quad (1)$$

Where each $\mathcal{L}_i : \mathbb{R}^\Theta \rightarrow \mathbb{R}$ is the risk function of the i -th client, of the form:

$$\mathcal{L}_i(\theta) := \mathbb{E}_{x \sim \mathcal{D}_i} [\ell_i(x; \theta)] \quad (2)$$

For some family of local losses $\ell_i : \mathbb{R}^d \times \mathbb{R}^\Theta \rightarrow \mathbb{R}$ and (not necessarily identical) data distributions \mathcal{D}_i . Some authors will specify \mathcal{L} to be weighted average of the local losses, but we assume that the average is unweighted and any client weightings w_i are subsumed in the definition of the local losses ℓ_i .

In the *federated* paradigm for optimisation, no client divulges knowledge of its data distribution by directly communicating its training data to any other participant. Instead, the aggregator queries each client by sending a set of parameters, and the client responds with an update based on local training against \mathcal{D}_i , which is then integrated into the global model. In the *synchronous* setting, the aggregator sends the same model to all selected clients and waits for responses from every participant before broadcasting the updated global model. In the *asynchronous* setting however, no client waits on any other, instead updates are aggregated as soon as they are received, and the next query dispatched to the updater client as soon as possible.

An early and archetypal example of an asynchronous algorithm is FEDASYNC (Xie et al., 2020), where each client receives the global parameters Θ^t and runs local SGD iterations to minimise the modified loss:

$$g_i(x; \theta) := \ell_i(x; \theta) + \frac{\mu}{2} \|\theta - \Theta^t\|^2 \quad (3)$$

Where, similar to the (synchronous) FEDPROX algorithm (Li et al., 2020), $\mu \in [0, 1]$ is a hyperparameter controlling the weight of the loss' *proximal term*. Once trained, the local parameters Θ_i^t are returned to the server, and the new global model is computed according to an exponential moving average for some learning rate schedule $\alpha_i^\tau \in \mathbb{R}_{\geq 0}$:

$$\Theta^{\tau+1} \leftarrow (1 - \alpha_i^\tau) \Theta^\tau + \alpha_i^\tau \Theta_i^t \quad (4)$$

Note that here, t denotes the global time step at which client i last received an updated global model, and τ the time step at which the server receives the latest update from the same client. In the synchronous case, we would have that these are always equal, and the global time step advances only once per entire server round.

Note a contrast between Equation 4 and the update rule of Asynchronous SGD (ASGD) (Dean et al., 2012):

$$\Theta^{\tau+1} \leftarrow \Theta^\tau - \eta_i^\tau \nabla_{\theta} \mathcal{L}_i(\Theta^t) \quad (5)$$

for some learning rate $\eta_i^t \in \mathbb{R}_{\geq 0}$. More generally, we can consider any *pseudo-gradient* $\Delta_{\theta} \mathcal{L}_i(\Theta^t) := \Theta^t - \Theta_i^t$ update for local optimisers other than SGD. Similar to FEDAVG and FEDSGD in the fully synchronous setting, in the case where the clients send and receive updates in a synchronous fashion (each client computes

the pseudo-gradient against the same global parameters and all updates from one set of parameters are aggregated before any updates are received from the next set) it is clear that these rules are equivalent. Assuming that client updates are processed in order of their index i , for $\tau = t + k$ with $k < N$:

$$(1 - \alpha)\Theta^\tau + \alpha\Theta_i^t = (1 - \alpha)^{k+1}\Theta^t + \sum_{i=0}^k (1 - \alpha)^{k-i}\alpha \cdot [\Theta^t - \Delta_{\theta}\mathcal{L}_{i+1}(\Theta^t)] \quad (6)$$

$$= \Theta^t - \sum_{i=0}^k \alpha(1 - \alpha)^{k-i} \cdot \Delta_{\theta}\mathcal{L}_{i+1}(\Theta^t) \quad (7)$$

Which is precisely the ASGD update with decaying learning rate $\eta_i^\tau = \alpha(1 - \alpha)^{k-i}$. Asynchronicity removes the guarantee used in Equation 6 that each client shares the same t and that $\Theta^\tau - \Theta^{t_i}$ is the sum of at most one single-step update from each client. Each of ASGD and FEDASYNC hence choose a different way of approximating the “true” update $\Delta_{\theta}\mathcal{L}_i(\Theta^\tau)$ from the delayed $\Delta_{\theta}\mathcal{L}_i(\Theta^{t_i})$. We contextualise these choices through the lens of Delay-Corrected ASGD (DC-ASGD) (Zheng et al., 2020).

The ASGD approach trusts learned displacements. In other words, we make the simplest possible approximation of the (unweighted) change to the global mode:

$$\Delta_{\theta}\mathcal{L}_i(\Theta^\tau) \approx \Delta_{\theta}\mathcal{L}_i(\Theta^{t_i}) \quad (8)$$

The FedAsync approach trusts learned positions. In other words, we use the update that maps $\Theta^\tau \mapsto \Theta^{t_i} - \Delta_{\theta}\mathcal{L}_i(\Theta^{t_i})$:

$$\Delta_{\theta}\mathcal{L}_i(\Theta^\tau) \approx \Delta_{\theta}\mathcal{L}_i(\Theta^{t_i}) + (\Theta^\tau - \Theta^{t_i}) \quad (9)$$

In this form, we consider the resemblance to the Taylor expansion of $\Delta_{\theta}\mathcal{L}_i$ around Θ^τ :

$$\Delta_{\theta}\mathcal{L}_i(\Theta^\tau) = \Delta_{\theta}\mathcal{L}_i(\Theta^{t_i}) + \nabla_{\theta}\Delta_{\theta}\mathcal{L}_i(\Theta^{t_i})(\Theta^\tau - \Theta^{t_i}) + \mathcal{O}\left(\left(\Theta^\tau - \Theta^{t_i}\right)^2\right) \mathbf{1}_D \quad (10)$$

Where $\mathbf{1}_D$ denotes the D -dimensional all-ones vector. This gives us that FEDASYNC can be thought of as a first-order Taylor approximation (*linearisation*) for the pseudo-gradient, on the assumption that the update function has a constant slope of 1. Where the local optimiser used is SGD, this is equivalent to the assumption that the loss surface has a constant curvature of 1 around modes.

The DC-ASGD approach uses a more complete version of the first-order Taylor expansion:

$$\Delta_{\theta}\mathcal{L}_i(\Theta^\tau) \approx \Delta_{\theta}\mathcal{L}_i(\Theta^{t_i}) + \nabla_{\theta}\Delta_{\theta}\mathcal{L}_i(\Theta^{t_i})(\Theta^\tau - \Theta^{t_i}) \quad (11)$$

Since the computation of the full Jacobian of $\Delta_{\theta}\mathcal{L}_i$ (equivalently the Hessian of \mathcal{L}_i where the local optimiser is SGD) would be quadratic in D , the DC-ASGD paper proposes that only the diagonal elements be considered. As opposed to work such as Yao et al. (2021) which uses an exact method such as Hutchinson’s to compute the Hessian diagonal, it is instead approximated as the diagonal of the simple unbiased estimator $\nabla_{\theta} \cdot (\nabla_{\theta})^\top$:

$$\nabla_{\theta}\mathcal{L}_i(\Theta^\tau) \approx \nabla_{\theta}\mathcal{L}_i(\Theta^{t_i}) + \lambda \cdot \text{diag}\left(\nabla_{\theta}\mathcal{L}_i(\Theta^{t_i}) \odot \nabla_{\theta}\mathcal{L}_i(\Theta^{t_i})\right) (\Theta^\tau - \Theta^{t_i}) \quad (12)$$

For some variance control parameter $\lambda \in \mathbb{R}_{>0}$.

2.3 Riemannian SGD

Recall that a smooth manifold $M \cong V \in \mathcal{P}(\mathbb{R}^n)$ is **Riemannian** if it is equipped with a positive-definite inner product $\langle \cdot, \cdot \rangle_p : T_p M \times T_p M \rightarrow \mathbb{R}$ on the tangent spaces at any point p (Lee, 2006). Recall further that the **exponential map** on a Riemannian manifold associates

$$\exp_p(v) : T_p M \longrightarrow M, \quad v \longmapsto \gamma_v(1) \quad (13)$$

Where $\gamma_v : [0, 1] \rightarrow M$ is the unique geodesic with initial tangent $\gamma'(0) = v$. From now on, we will use “Riemannian manifold” to refer to those Riemannian manifolds which are **geodesically-connected**, meaning that for any $x, y \in M$ there exists a geodesic $\gamma : [0, 1] \rightarrow M$ such that $\gamma(0) = x, \gamma(1) = y$. By the Hopf-Rinow theorem, **geodesic completeness** (that $\exp_p(v)$ is well-defined for all $p \in M, v \in T_p M$) is a sufficient but not necessary condition.

Recalling that SGD can be equivalently formulated as stepping along the Euclidean geodesic in \mathbb{R}^Θ in the direction of the tangent $\nabla \mathcal{L}(\Theta)$, **Riemannian SGD** (Bonnabel, 2013) refers to the simple observation that we may generalise such a procedure to arbitrary submanifolds which more accurately capture the loss function geometry (subject to mild regularity conditions). To the best knowledge of the authors, there is no framework in the literature which makes these same generalisations to each step of the (async) FL process and provides convergence guarantees in this setting, as we do with ASYNCMANIFOLD in Section 5.1.

2.3.1 Pseudo-Gradients on Riemannian Manifolds

Notating $\pi_M : \mathbb{R}^\Theta \rightarrow M$ as a continuous projection onto M and $\|\cdot\|_M$ as a norm, in Section 5.1, we will want to be able to define a proximal term:

$$\|\pi_M(\theta) - \pi_M(\Theta)\|_M^2 =: \|\Delta_\pi \mathcal{L}(\Theta)\|_M^2 \quad \text{where } \Delta_\pi \mathcal{L}(\Theta) \text{ is a } \textit{pseudo-gradient} \text{ update} \quad (14)$$

Where the local optimiser is full-batch GD on M (using the *Riemannian GD* formulation of Nickel & Kiela (2018)), we have that $\|\cdot\|_M = \|\cdot\|_\Theta$ - the Riemannian norm at Θ - will be well-defined, as the update is guaranteed to be $\in T_\Theta M$. In the case where a different local optimiser is used (including mini-batch SGD), it is possible that this will no longer hold. A norm on pseudo-gradients is still guaranteed to exist but, in this case, it must be defined via a Riemannian version of the Mean Value Theorem. In particular, there will exist some point $t \in [0, 1]$ on the geodesic $\gamma : [0, 1] \rightarrow M$ such that $\gamma(0) = \Theta$ and $\gamma(1) = \theta$ where the tangent to the curve $\in T_{\gamma(t)} M$ is of the form $\lambda \Delta_\pi \mathcal{L}(\Theta)$ for some $\lambda \in \mathbb{R}_{>0}$. Accordingly, there is some speed reparametrisation $\hat{\gamma}$ of γ such that the tangent at $\hat{\gamma}(t) = \Delta_\pi \mathcal{L}(\Theta)$, and hence we have that $\Delta_\pi \mathcal{L}(\Theta) \in T_{\hat{\gamma}(t)} M$ so $\|\cdot\|_M = \|\cdot\|_{\hat{\gamma}(t)}$ is defined.

This formulation of $\|\cdot\|_M$ is not, however, always well-defined. In particular, the same tangent vector may be assigned different values by the Riemannian norm at different points, and a given geodesic might have multiple points where the angle between tangent and $\Delta_\pi \mathcal{L}(\Theta)$ is zero. To account for this case, a pseudo-gradient implementation should define a *uniform* Riemannian metric - $\forall p \in M, \langle \cdot, \cdot \rangle_p = \langle \cdot, \cdot \rangle_M$ - as we will see, this assumption also enables the analysis w.r.t. the ambient manifold of Theorem 1.

3 Orthogonal Delay Correction

We notice that each methodology presented in Section 2.2 through the DC-ASGD lens of the Taylor linearisation can be expressed in more direct linear-algebraic terms as members of the following class of delay correction algorithms:

$$\Delta_i^\tau \approx \Delta_i^{t_i} + \lambda_i^{t_i, \tau} \cdot \mathbf{M}_i^{t_i, \tau} \cdot (\Theta^\tau - \Theta^{t_i}) \quad (15)$$

For some functions of matrices $\mathbf{M} \in \mathbb{R}^{\Theta \times \Theta}$ and coefficients $\lambda \in [0, \infty)$. Note that we do not here include any notions of “staleness” by which the weighting of a delayed update is reduced, as this is subsumed into an adaptive learning rate of the respective algorithm. We have so far encountered:

$$\begin{aligned} \lambda_i^{t_i, \tau} = 0 & & \mathbf{M}_i^{t_i, \tau} = \mathbf{I}_d & & \text{(ASGD)} \\ \lambda_i^{t_i, \tau} = 1 & & \mathbf{M}_i^{t_i, \tau} = \mathbf{I}_d & & \text{(FEDASYNC)} \\ \lambda_i^{t_i, \tau} = \lambda & & \mathbf{M}_i^{t_i, \tau} = \text{diag}(\Delta_i^{t_i})^2 & & \text{(DC-ASGD)} \end{aligned}$$

This motivates considering a solution to the delay correction problem by choosing $\mathbf{M} = \mathbf{I}_d$ and finding an optimal linear combination of $\{\Delta_i^{t_i}, \Theta^\tau - \Theta^{t_i}\}$. In keeping with the spirit of this paper, we seek an approach that considers the optimisation trajectories in a *geometric* way. One method deployed successfully in multi-task learning is the (sequential) **Gradient Surgery** approach of Yu et al. (2020). This algorithm considers

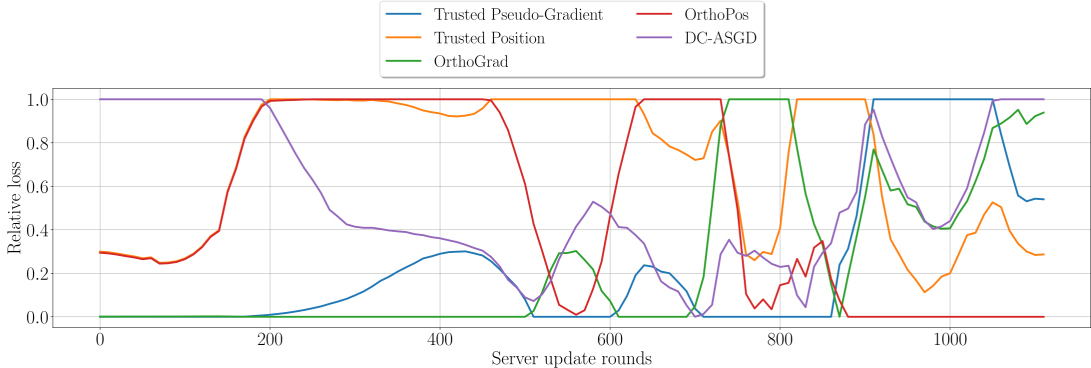


Figure 1: Smoothed global test loss at each server round of asynchronous federated LeNet-5 training for a selection of endpoint delay-correction methods

client updates Δ_1, Δ_2 to “conflict” if they have an obtuse angle between them (i.e. $\Delta_1 \cdot \Delta_2 < 0$). Where updates conflict, Δ_1 will be projected into the orthogonal complement subspace of Δ_2 , hence any action of Δ_1 in direct opposition to Δ_2 will be cancelled, whilst preserving orthogonal movement.

Inspired by this work, we propose the ORTHOCORRECT algorithm for delay correction, for tunable hyperparameters $\alpha \in \mathbb{R}, \vartheta \in [-1, 1]$:

$$\lambda_i^{t_i, \tau} = \begin{cases} \text{scalarProj}_{(\Theta^{t_i} - \Theta^\tau)}(\Delta_i^{t_i}) & \cos\text{Angle}(\Delta_i^{t_i}, \Theta^{t_i} - \Theta^\tau) \leq \vartheta \\ \alpha & \text{otherwise} \end{cases} \quad \mathbf{M}_i^{t_i, \tau} = \mathbf{I}_d \quad (\text{ORTHO CORRECT})$$

Where $\text{scalarProj}_{\mathbf{b}}(\mathbf{a}) := \frac{\mathbf{a} \cdot \mathbf{b}}{\|\mathbf{b}\|}$, $\cos\text{Angle}(\mathbf{a}, \mathbf{b}) := \frac{\mathbf{a} \cdot \mathbf{b}}{\|\mathbf{a}\| \|\mathbf{b}\|}$.

The (ORTHO CORRECT) equation where $\alpha = \vartheta = 0$ (termed ORTHOGRAD) is equivalent to gradient surgery with $\Delta_1 = \Delta_i^{t_i}$ and $\Delta_2 = (\Theta^{t_i} - \Theta^\tau)$ (note that we are projecting onto the *negative* movement of the global mode). A simple rearrangement shows that $\alpha = 1$ (termed ORTHOPOS) gives gradient surgery where $\Delta_1 = \Delta_i^{t_i} + (\Theta^\tau - \Theta^{t_i})$. Where $\vartheta = 1$ (ORTHO STRICT), we consider only movement of the local mode orthogonal to the movement of the local mode, regardless of “conflict”, making the ASGD/FEDASYNC approaches equivalent.

To the best knowledge of the authors, no thorough comparative study exists in the literature of the local (geometric) behaviour of delay correction proposals, with existing work (Zheng et al., 2020; Shi et al., 2025) considering only the performance of models trained with each proposal at convergence, despite it being *local* behaviour that primarily appears in convergence results (notably Theorem 1). To inform choice of delay-correction method in the algorithmic framework of Section 5.2, we go some way to rectifying this.

For these experiments, we run both FEDASYNC and our proposal ASYNCCURVE with no delay correction. The data is divided amongst clients $\{1, \dots, 8\}$, with heterogeneity simulated by giving each client a number of training examples proportional to its index. We train a LeNet-5 (Lecun et al., 1998) on the FEMNIST dataset (Caldas et al., 2019). At each server update step, a model checkpoint is saved with details of the contributing client, and methodologies are evaluated by a later sweep through the checkpoints, measuring the step-wise train/val/test losses of the proposal. DC-ASGD is implemented with the adaptive λ parameter suggested in Zheng et al. (2020), scaled by a factor of 2.5 in order to ensure a significant enough difference from the trusted p-grad method. To generate the plots, losses are smoothed by convolution with a Gaussian filter ($\sigma = 100$, truncated after 2σ); normalised relative losses $\in [0, 1]$ are then computed and averaged over the underlying federated algorithms.

Figure 1 shows the test loss performance of each endpoint delay correction method over time for the LeNet-5 training. The most striking feature of this plot is the dominance of pseudo-gradient-trusting methods in the

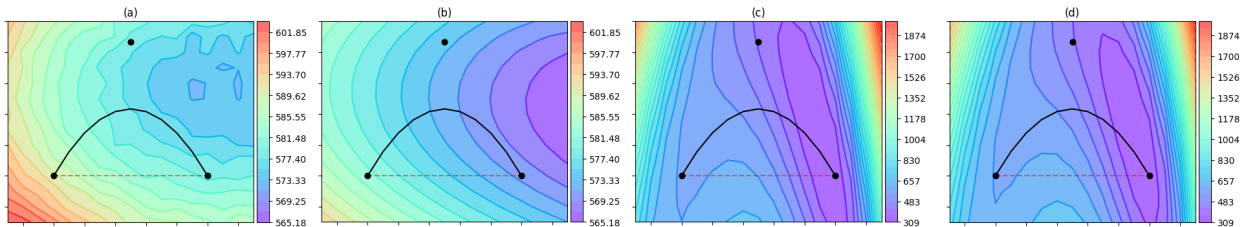


Figure 2: Quadratic Bezier mode connections learned during the federated training of LeNet-5, projected onto a 2-d loss landscape. Plot (a) shows cross-entropy loss w.r.t. a local training set and (b) w.r.t. the global test set where the local mode has been trained for 10 epochs. Plots (c) and (d) show the training and test losses respectively where the local mode has been trained for 250 epochs.

earlier stages of training, switching to the dominance of position-trusting methods in the latter stages. This makes intuitive sense: as the training progresses to convergence, steps become smaller and more precise and the optimisation trajectory often begins “circling” a minimum. Here, making steps towards a point that is known to be low-loss becomes (at least in the local view) superior to inferring a point that may be low-loss based on a delayed gradient. This discovery suggests that it is most useful not to use the same method of delay-correction over the entire run, but to dynamically adapt to the local geometry of the loss landscape, using closeness to convergence as a proxy statistic.

Another feature to note is the dominance of ORTHOCORRECT when applied to the corresponding “best” method for a particular point during convergence (except in the region around the phase transition), suggesting a delay correction we refer to as ORTHODYN which progresses:

$$\text{ORTHOGRAD} \longrightarrow (\text{Optional: ASGD}) \longrightarrow \text{ORTHOPOS} \quad (16)$$

When this transition occurs can be chosen based on any statistic which captures useful information about the local loss landscape.

We note that DC-ASGD, while never the optimal choice, can be seen as a weighted average of the gradient- and position-based methods, and accordingly spends much of the run with performance somewhere between the two (although hyperparameter tuning is required to ensure the right amount of correction is performed). The observed superior performance of the algorithm over ASGD in Zheng et al. (2020) may thus be attributable to this “compromise”, which would in turn suggest favouring a dynamic approach over DC-ASGD.

4 Quadratic Mode Connections and Curvature Transference

Recall that the *Linear Mode Connectivity* hypothesis asserts that independent neural network minima are often connected by straight lines of low-loss, but that this often fails to hold, although they may still be connected by polynomial curves (Lubana et al., 2023). Some authors consider a stronger hypothesis that extends to entire low-loss submanifolds (Benton et al., 2021), but we instead make a natural generalisation: that there exists a manifold on which the geodesic connection of minima is low-loss. In particular, this subsumes the *Polynomial Mode Connectivity* hypothesis, as we notice that the graph of a Bezier curve is a 1-dimensional submanifold, on which the geodesics trivially follow the polynomial in \mathbb{R}^Θ . We consider, therefore, a *proof-of-concept* choice of learnable \mathcal{M}_g for ASYNCMANIFOLD based on 1-dimensional quadratic Bezier (QB) curves. For this, we must establish the expected value of the manifold quality parameter Q (see Theorem 1). We proceed in two stages: first establishing QB curves as superior to linear connections in the synchronous setting, before investigating whether the curvature learned against a delayed pseudo-gradient in the async setting is *transferable* to its delay corrected counterpart.

Figure 2 shows the advantage of taking into account curvature and learning quadratic mode connections via a control point orthogonal to the linear connection. In all four cases, we see that moving a given Euclidean distance from the global mode along the quadratic connection will yield a loss lower than moving the same

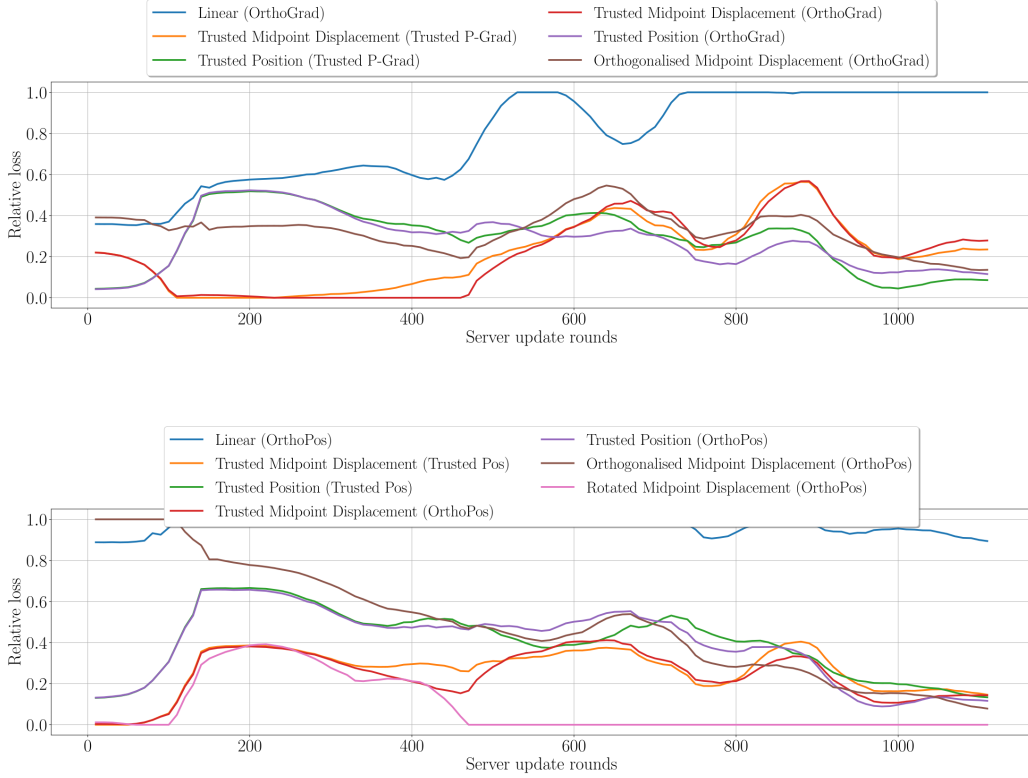


Figure 3: Smoothed global test loss at each server round of asynchronous federated LeNet-5 training for a selection of control point delay correction methods

distance along the linear connection. In particular, plots (c) and (d) show a configuration reminiscent of figures in Garipov et al. (2018), where the longer local training time has allowed the optimisation trajectory to navigate around an “obstruction” in parameter space of higher loss that is encountered when moving along the linear connection, but is avoided by the quadratic curve.

In Figure 3, we extend the analysis of the previous section to the performance of Bezier curves where the learned control point is similarly delayed. We test different approaches to delay-correcting the control point, evaluating the loss along the quadratic connection induced from both gradient- (top) and position- (bottom) based endpoint correction. The control points were learned in 5 epochs of training with the Adam optimiser at learning rate $\eta = 10^{-4}$ (10x smaller than for the endpoints).

These plots confirm our previous explorations that the learned quadratic connection will consistently outperform the linear one. Furthermore, it shows that the curvature learned with respect to a delayed connection is robust enough that it continues to improve performance when acting on an updated line. We refer to this as the property of *curvature transference*.

As may be expected, we notice the same phenomenon of a gradient \rightarrow position phase change as training progresses, occurring at the same point as the transition began in Figure 1. Notable from the lower plot is the clear dominance of *rotational delay correction*. Denote by $\varphi \in \mathbb{R}^\Theta$ the control point learned w.r.t. the $\Theta^t \mapsto \Theta_i^t$ linear connection. Now suppose $\hat{\Theta}_i^\tau$ is the delay-corrected local mode and R is a rotation matrix that aligns the local update vector $-\Delta^\tau := \Theta_i^t - \Theta^t$ with the delay-corrected update $\hat{\Theta}_i^\tau - \Theta^\tau$. Then we define:

$$\varphi_{\text{rot}} := \frac{\Theta^\tau + \hat{\Theta}_i^\tau}{2} + R \left(\varphi - \frac{\Theta^t + \Theta_i^t}{2} \right) \quad (17)$$

In words, we simply rotate the learned displacement of the control point so the angle between linear connection and control point is preserved. In Figure (3), this is applied only to positional methods as we note that, where the underlying endpoint correction is trusted pseudo-gradient, R will be the identity matrix. In practice, to keep the complexity linear in the dimension of \mathbb{R}^Θ , we perform the rotation by first projecting displacements into the plane spanned by the two pseudo-gradients, performing the rotation in 2D, and finally adding back the orthogonal complement of the projected displacement.

Whilst this represents a substantial margin in terms of relative loss, the methods are tightly bunched in absolute terms, especially as convergence is reached. We find an estimated $Q \approx 1.0275$ on test loss (99% Gaussian CI ± 0.0139), which still represents a consistent non-negligible improvement in performance.

5 The AsyncManifold Algorithms

With this background and exploratory work established, we may now set out our framework for Riemannian asynchronous aggregation. We begin by describing the general ASYNCMANIFOLD family of algorithms, before presenting our particular proposal, inspired by Garipov et al. (2018), leveraging quadratic Bezier mode connections as the (1-dimensional) client-side learnable manifold.

5.1 AsyncManifold

Recall that ℓ_i denotes the loss function of client i , with \mathcal{L}_i the corresponding risk. Similarly, let $F_i(\cdot | \Theta)$ denote \mathcal{L}_i with the proximal term added w.r.t Θ (omitted where unambiguous). Let \mathcal{L} denote the weighted average global loss.

Client Operations Upon receiving a Θ^t from the server, client i should perform a local optimisation step to solve

$$\min_{\theta} F_i(x; \theta, \Theta^t) := \ell_i(x; \theta) + \frac{\mu}{2} \|\pi_{\mathcal{M}_0}(\theta) - \pi_{\mathcal{M}_0}(\Theta^t)\|_{\mathcal{M}_0}^2 \quad (18)$$

Where $\pi_{\mathcal{M}_0}, \|\cdot\|_{\mathcal{M}_0}$ are defined as in Section 2.3. Depending on the choice of \mathcal{M}_0 , the proximal term may be computed by first projecting $\pi(\theta) - \pi(\Theta^t)$ onto the tangent space $T_{\Theta^t}\mathcal{M}_0$. The choice of optimisation algorithm and Riemannian manifold \mathcal{M}_0 can vary between implementations; for $\mathcal{M}_0 = \mathbb{R}^\Theta$ we recover the traditional FEDPROX objective, and we find the objective used in FEDMRUR (An et al., 2023) by letting \mathcal{M}_0 be the hyperbolic space and $\|\cdot\|_{\mathcal{M}_0}$ be the exponentiated square Lorentzian distance (see Section 5.2 for a detailed definition). Furthermore, the local solver is not restricted to performing gradient steps in Euclidean ambient space, and may instead compute the gradient and step along geodesics (Bonnabel, 2013) in any well-chosen ambient Riemannian manifold (see Assumption 8), including \mathcal{M}_0 directly. A notable example here would be the use of hyperbolic SGD in Nickel & Kiela (2018). In the results of Section 5.1.2, we provide convergence guarantees w.r.t. the norm on this ambient manifold.

Since the ASYNCMANIFOLD algorithm is geometric in nature, implementations may wish to choose a local optimiser which seeks to improve generality by encouraging trajectories towards flat minima - most notably the (Adaptive) Sharpness-Aware Minimisation family of algorithms (Foret et al., 2021; Kwon et al., 2021), as exemplified by Caldarola et al. (2022). A detailed theoretical analysis of convergence where non-SGD solvers are used, however, is left to future work.

Once a local mode Θ_i^t has been learned, the client should choose a low-dimensional Riemannian parametric manifold $\mathcal{M}_\varphi \cong \mathbb{R}^n$ for some $1 \leq n \ll D$ (note that the space of parameters φ need not be low-dimensional, only \mathcal{M}_φ). φ_i^t should be an approximate solution to:

$$\min_{\varphi} \int_{\mathcal{M}_\varphi} \mathbb{E}_{x \sim \mathcal{D}_i} [\ell_i(x; \theta)] d\theta = \mathbb{E}_{\theta \sim U(\mathcal{M}_\varphi)} [\mathcal{L}_i(\theta)] \quad (19)$$

The manifold should be of low \mathcal{L}_i loss such that $\Theta^t, \Theta_i^t \in \mathcal{M}_\varphi$. The choice of parametric family and parameter optimisation method is again left as an implementation decision. Although we have presented these two steps as sequential, it is likely beneficial for an algorithm to learn φ jointly with Θ_i^t - for example, optimising φ for

one epoch after each epoch optimising spent Θ_i^t . This approach also enables an ASYNCMANIFOLD algorithm to incur no extra cost in client wall-clock time as training each parameter can be conducted in parallel.

With each component optimised, the client sends the update triple $\langle t, \theta_i^t, \varphi_i^t \rangle$.

Server Operations Upon receiving $\langle t, \Theta_i^t, \varphi_i^t \rangle$ at server time step τ , the server should perform a delay-correction to yield estimated $\hat{\Theta}_i^\tau, \hat{\varphi}_i^\tau$. The method is left unspecified in general, as it will likely depend on the parametric manifold families chosen, but we direct the reader to Section 3 for a detailed discussion. From here, the server should choose a Riemannian manifold \mathcal{M}_g from which to draw the next global mode, such that $\Theta^\tau, \hat{\Theta}_i^\tau \in \mathcal{M}_g$. This chosen manifold should approximately minimise the *global* loss \mathcal{L} , in much the same way as \mathcal{M}_φ is chosen according to the *local* loss \mathcal{L}_i in Equation (19). In general, the server will have access to information about each local loss surface (hence the global loss surface) only via the history of updates from each client, so a low-loss \mathcal{M}_g cannot be learned directly and instead must be approximated from the parameters learned at each client.

Finally, we exploit geodesic connectivity to find the unique $\gamma^\tau : [0, 1] \rightarrow \mathcal{M}_g$ connecting Θ^τ and $\hat{\Theta}_i^\tau$, denoting $(\gamma^\tau)'(0) =: \mathbf{T}^\tau$. The server then chooses a step size $\eta^\tau \in [0, 1]$ and scales \mathbf{T}^τ accordingly. A crucial note here about the adaptive global learning rate is the use of a *dominance penalty* to encourage client fairness inspired by Leconte et al. (2024). Letting I_τ denote the random variable which corresponds to the client index at round τ , the server maintains \mathbf{p} , the empirical distribution of I and scales $\eta_g^{(\tau)} = \frac{1}{N p_{i_\tau}} \eta_g$ - we write p_{i_τ} , but note that this probability will be dependent on the time since the last update was received from i_τ . We update Θ :

$$\Theta^{\tau+1} \leftarrow \exp_{\Theta^\tau}(\eta_g^{(\tau)} \cdot \mathbf{T}^\tau) \quad (20)$$

Equivalently, we re-parametrise the speed at which γ^τ is traversed, so the exponential map returns a point after “less than one unit” of travel on the original γ^τ . before setting $\Theta^{\tau+1} \leftarrow \gamma^\tau(\eta^\tau)$. A momentum-based displacement $m^\tau : \mathcal{M}_g \rightarrow \mathcal{M}'_g$ may be applied to $\Theta^{\tau+1}$ here - depending on the computational requirements of the server and the geometry of the problem, it may be more efficient to apply momentum directly in Euclidean space ($\mathcal{M}'_g = \mathbb{R}^\Theta$), but geometric information should be preserved ($\mathcal{M}'_g = \mathcal{M}_g$) where possible.

Stochastic Weight Averaging (Izmailov et al., 2019) may be used and if $\tau \equiv 0 \pmod{c}$ (where c is the cycle length), the updated Θ^{SWA} is computed here. For the “Periodic” flavour (Guo et al., 2022), if $\tau \equiv 0 \pmod{C}$ (where C is the long cycle length), we overwrite $\Theta^{\tau+1} \leftarrow \Theta^{\text{SWA}}$. Note that we assume a no-centralised data setting, so the low-loss manifold on which SWA is performed is approximated by a single simplex - indeed, this is a linearisation of the Fast Geometric Ensembling approach (Garipov et al., 2018) and is justified by the observations in the aforementioned literature that performance is often comparable.

5.1.1 The AsyncManifold lens on existing methods

It is clear that methods inheriting from standard FEDAVG (regardless of delay-correction method used) are immediately recovered as ASYNCMANIFOLD algorithms by setting $\mathcal{M}_\varphi = \mathcal{M}_g = \mathbb{R}^\Theta$ and hence considering the trivial parametrisation $\varphi \in \mathbb{R}^0$. To see this, note that applying an update Δ^τ with some learning rate η is exactly using $\Theta^{\tau+1} \leftarrow \gamma(\eta)$ where γ is the linear interpolation:

$$\gamma(\eta) = \Theta^\tau + \eta([\Theta^\tau - \Delta^\tau] - \Theta^\tau) \quad (21)$$

Straight lines are trivially the geodesics in the Euclidean space \mathbb{R}^Θ with the canonical Riemannian metric (Lee, 2006).

Some methods in the mode connectivity literature seek to extend the learning of 1-dimensional paths to the learning of manifolds, and in many cases this is manifested as learning low-loss *simplicial complexes* (Benton et al., 2021). Unfortunately, existing methods employing these insights in the federated setting often restrict this to learning single simplexes, inspired by the *linear* flavour of mode connection. Crucially, this forces the learned manifolds to have zero curvature, losing much of the geometric information we seek to exploit in ASYNCCURVE. A notable example from synchronous FL would be FLOCO (Grinwald et al., 2025), which

is not strictly an ASYNCMANIFOLD algorithm, but fits into our framework by each client learning n models, acting as endpoints of a simplex. In the first step of the algorithm, we set:

$$\begin{aligned} \Phi \in \mathbb{R}^{n \times D} \quad \mathcal{M}_\Phi &= \left\{ \sum_{i \in [n]} \lambda_i \Phi_i \mid \sum_{i \in [n]} \lambda_i = 1 \text{ and } \forall i, \lambda_i \in [0, 1] \right\} \\ \hat{\Phi} := \text{round-wise mean of client } \Phi\text{s} \quad \mathcal{M}_g &= \left\{ \sum_{i \in [n]} \lambda_i \hat{\Phi}_i \mid \sum_{i \in [n]} \lambda_i = 1 \text{ and } \forall i, \lambda_i \in [0, 1] \right\} \end{aligned}$$

Later steps will restrict the values that $\{\lambda_i\}_{i \in [n]}$ can take on a per-client basis, but still follow the same choice of parametric family. Synchronous methods do no delay correction, so we write that FLOCO considers a single update $\hat{\Theta}^\tau$ aggregated over clients, which is chosen as the centroid of \mathcal{M}_{Φ^τ} . As usual in the synchronous setting, FLOCO concludes by setting $\Theta^{\tau+1} = \gamma(1) = \hat{\Theta}^\tau$.

5.1.2 Convergence Insights

We can now provide our main result, a general convergence proof of SGD-based algorithms within the ASYNCMANIFOLD framework, subject to reasonableness constraints on the choice of manifolds.

We begin with some standard assumptions of non-convex optimisation:

Assumption 1 (*L-Smoothness of Loss Functions*). *Each client risk is L_R -smooth: $\forall x, y \in \mathbb{R}^\Theta$, $\|\nabla \mathcal{L}_i(x) - \nabla \mathcal{L}_i(y)\| \leq L_R \|x - y\|$. We also require smoothness of the projection onto an orthonormal (with respect to $\|\cdot\|_{\mathcal{M}_0}$) basis of \mathcal{M}_0 . In particular: $\forall x, y \in \mathbb{R}^\Theta$, $\|\nabla \pi_{\mathcal{M}_0}(x) - \nabla \pi_{\mathcal{M}_0}(y)\| \leq \frac{L_N}{2} \|x - y\|$. Hence $\|\pi_{\mathcal{M}_0}(\cdot)\|_{\mathcal{M}_0}$ is L_N -smooth.*

Assumption 2 (*Bounded Variance*). *Each client i may query an oracle for g_Θ^i , distributed as an unbiased estimator for $\nabla F_i(\Theta)$. This should satisfy: $\forall \Theta \in \mathbb{R}^\Theta$, $\mathbb{E} \|g_\Theta^i - \nabla F_i(\Theta)\|^2 \leq \sigma_i^2$. This should also satisfy that $\mathbb{E} \|g_\Theta^i - \nabla F(\Theta)\|^2$ is suitably bounded, but we do not introduce an explicit quantity.*

Assumption 3 (*Bounded Gradients*). *There exists G such that, for all i , F_i has gradient bounded by G : $\forall x \in \mathbb{R}^\Theta$, $\|\nabla \mathcal{L}_i(x)\| \leq G$. Similarly, we require that $\forall x \in \mathbb{R}^\Theta$, $\|\nabla F_i(x)\| \leq G_2$.*

We make a standard assumption on the “niceness” of our setting and the fairness of client participation:

Assumption 4 (*Bounded Staleness*). *Suppose an update from client i arrives at time τ , with the local copy of the client model being Θ^t . Then $\mathbb{E} [\|\Theta^\tau - \Theta^t\| \mid \Theta^t] \leq S \max_{t' \in [t.. \tau-1]} \mathbb{E} [\|\Theta^{t'+1} - \Theta^{t'}\| \mid \Theta^{t'}]$. Note that $\tau - t \leq S$ immediately implies this constraint via the triangle inequality.*

Assumption 5 (*Ergodic Client Participation*). *As $T \rightarrow \infty$, each client should participate in updates infinitely often, and indeed the proportion of updates performed by each client (p_i) should be bounded below above 0. The distribution \mathbf{p} should converge to stationary and hence the empirical CDF converges to unbiased estimation for T large enough. We assume that observations of the client index RV are independent, when conditioned on the time since the last update.*

We quantify the “reasonableness” of the manifolds chosen:

Assumption 6 (*Bounded Manifold Quality*). *Let γ denote the geodesic in \mathcal{M}_g such that $\gamma(0) = \Theta^t$, $\gamma(1) = \Theta^{t+1}$, and let $\hat{\gamma}$ denote their linear interpolation. Then the loss at a point a given step length along γ should be at least Q times better than at the same point along $\hat{\gamma}$: $\forall \lambda \in [0, 1]$, $\mathbb{E}[F(\gamma(\lambda)) \mid \Theta^t] \leq \frac{1}{Q} \mathbb{E}[F(\hat{\gamma}(\lambda)) \mid \Theta^t]$.*

Notice that any delay-correction method on the learning of the manifold is subsumed into this assumption.

Assumption 7 (*Bounded Geodesic Divergence*). *Let γ denote the geodesic in \mathcal{M}_g such that $\gamma(0) = \Theta^t$, $\gamma(1) = \Theta^{t+1}$, and let $\hat{\gamma}$ denote the same geodesic in the ambient manifold. Then the distance at a point a given step length along γ from the start point should be at most D times larger than at the same point along $\hat{\gamma}$: $\forall \lambda \in [0, 1]$, $\mathbb{E}[\|\gamma(\lambda) - \Theta^t\| \mid \Theta^t] \leq D \mathbb{E}[\|\hat{\gamma}(\lambda) - \Theta^t\| \mid \Theta^t]$.*

Finally, we restrict the choice of ambient manifold where it is non-Euclidean to ensure the convergence of Riemannian SGD:

Assumption 8 (Bounded Ambient Curvature). *The ambient manifold should have injectivity radius $I > 0$ and embed smoothly into Euclidean space. Furthermore, the norm of the second fundamental form α and its first derivative $\nabla\alpha$ should be uniformly bounded by $C \geq 0$.*

Note that Assumption (7) compares to the geodesic in the (not necessarily Euclidean) ambient manifold, but Assumption (6) always compares γ to the straight line.

Remark (The Meaning of ∇). *In the present work, we restrict our analysis to clients where the local solver is mini-batch SGD. In this sense, ∇ denotes some form of derivation. In the simplest case, where the ambient manifold is \mathbb{R}^Θ Euclidean space, we write $\nabla F(x) := (\nabla_{\mathbf{x}} F)|_x(x)$ for brevity - where \mathbf{x} denotes the parameters of F . For arbitrary ambient manifolds, we may use ∇ to denote the Levi-Civita connection. The proof may be generalised to adaptive mini-batch gradient methods following the style of Reddi et al. (2021).*

Let K denote the maximal number of local solver steps taken by each client (although the actual number taken may vary depending on time step and client, K is simply an upper bound). Since the trusted pseudo-gradient provides the most direct way to approach the convergence proof, this is what we restrict our analysis to here, and we leave finding improved convergence rates for delay corrected pseudo-gradients to future work. Similarly, our analysis does not extend to the case where Stochastic Weight Averaging is used, although only minor modifications to the proof are needed (especially due to the ergodic nature of the convergence rate).

Theorem 1 (Convergence of ASYNCMANIFOLD). *Suppose that at each server step s , the server receives an update from client i_s with local root model Θ^{t_s} . Subject to the assumptions above, with all symbols as defined therein, we find an ergodic convergence rate for T high enough, choosing the hyperparameters $\eta_g = \Theta(1), K = \Theta(1), \eta_l = \Theta(\frac{1}{\mu L_N K \sqrt{T}})$:*

$$\mathbb{E} \left[\frac{1}{T} \sum_{s=0}^{T-1} \|\nabla \mathcal{L}(\Theta^s)\|^2 \right] \leq \mathcal{O} \left(\frac{\mathcal{L}(\Theta^0) - Q\mathcal{L}(\Theta^*)}{T\sqrt{T}} + \Psi\sqrt{T} \right) + \mathcal{O} \left(\frac{4G^2 + \sigma_l^2}{\sqrt{T}} \right) \quad (22)$$

$$+ \mathcal{O} \left(\frac{(1 + S^2 D^2)(4G^2 + \sigma_l^2) + G^2 + G_2^4 C^2}{T} \right) + \mathcal{O} \left(\frac{G_2^6 C^2}{T^2} \right)$$

$$\text{where } \Psi = (1 - Q) \begin{cases} \min_t \mathcal{L}(\Theta^t) & \text{if } Q \geq 1 \\ \max_t \mathcal{L}(\Theta^t) & \text{otherwise} \end{cases} \quad (23)$$

Convergence as $T \rightarrow \infty$ is thus guaranteed for any choice of \mathcal{M}_g with $Q \geq 1$. The last asymptotic term is derived from the curvature bounds on the ambient manifold, and hence is zero and can be ignored when the ambient manifold is totally geodesic in Euclidean space. See Equation (69) for a rate that maintains the dependence on hyperparameters $\{K, \eta_l, \eta_g\}$.

For brevity, the detailed proof is deferred to Appendix A. It is immediate then that, for (quasi-)convex losses \mathcal{L}_i , the algorithm will converge to a global minimum. The generality (w.r.t. the unbiased client setting) in which the result is proved makes it quite powerful - one can, for example, immediately derive as a corollary a convergence result for FEDASYNC (with $D = Q = 1$, assuming the use of a dominance penalty) that does not place the strong constraints on μ of the proof found in Xie et al. (2020). Similarly, convergence in the synchronous setting is immediate with very minor modification to the proof, allowing us to drop the global drift terms. This does not mean, however, that future work cannot derive tighter bounds on the convergence rate, especially where certain manifolds (such as a non-Euclidean ambient manifold or \mathcal{M}_0) are fixed.

5.2 AsyncCurve

We describe ASYNCCURVE as an instance of ASYNCMANIFOLD, utilising *quadratic* mode connections.

Choice of optimisers Depending on the computational requirements of each client, we use either the Adaptive Sharpness-Aware Minimisation algorithm or the usual Adam optimiser (Kingma & Ba, 2017) on

the client-side, along with Periodic SWA on the server-side. The ambient manifold is simply Euclidean space, so we do not perform any Riemannian SGD steps.

Choice of \mathcal{M}_0 We follow FEDMRUR, using projection into the Lorentzian hyperbolic space with an exponential squared Lorentzian regularisation term. Accordingly, each client solves:

$$\min_{\boldsymbol{\theta}} F_i(x; \boldsymbol{\theta}, \Theta^t) := \ell_i(x; \boldsymbol{\theta}) + \frac{\mu}{2} \exp \left[\frac{1}{\sigma} \|\pi_L(\boldsymbol{\theta}) - \pi_L(\Theta^t)\|_L^2 \right] \quad (24)$$

Where here $\exp : x \mapsto e^x$ denotes the usual exponential map on \mathbb{R} , as opposed to a particular Riemannian exponential map and $\sigma \in \mathbb{R}_{>0}$ is a variance control hyperparameter. Letting $D = |\Theta|$, $\pi_L : \mathbb{R}^D \rightarrow \mathcal{H}^D$ defines a projection into the *Lorentz (hyperboloid) model* of hyperbolic space (Law et al., 2019):

$$\mathcal{H}^D := \{\mathbf{x} \in \mathbb{R}^{D+1} \mid \langle \mathbf{x}, \mathbf{x} \rangle_L = -\beta, \mathbf{x}_0 > 0\} \quad (25)$$

β here is technically a hyperparameter, but we use the canonical choice $\beta = 1$ (An et al., 2023; Nickel & Kiela, 2018). Here $\langle \cdot, \cdot \rangle_L$ denotes the *Lorentz inner product* on \mathcal{H}^D (note that this makes the chosen manifold \mathcal{M}_0 Riemannian as required):

$$\langle \mathbf{x}, \mathbf{y} \rangle_L := -\mathbf{x}_0 \mathbf{y}_0 + \sum_{i=1}^D \mathbf{x}_i \mathbf{y}_i \quad \|\mathbf{x}\|_L^2 := \langle \mathbf{x}, \mathbf{x} \rangle_L \quad (26)$$

It is clear then that we have:

$$\pi_L : \mathbf{x} \mapsto \left(\sqrt{\beta + \|\mathbf{x}\|^2}, \mathbf{x} \right) \quad (27)$$

Where $\|\cdot\|$ is the usual Euclidean norm on \mathbb{R}^D .

Choice of \mathcal{M}_φ Each \mathcal{M}_φ is the graph of a quadratic Bezier curve

$$\beta_\varphi^t : t \in [0, 1] \mapsto (1-t)^2 \Theta^t + t(1-t)\varphi + t^2 \Theta_i^t \quad (28)$$

The norm on the curve is defined by the norm in the parameter space $[0, 1]$, hence

$$\|\theta\|_{\mathcal{M}_\varphi} := \beta_\varphi^{-1}(\theta) \quad (29)$$

The control point $\varphi \in \mathbb{R}^\Theta$ is learned using the Adam optimiser by sampling a point along the curve at each mini-patch and propagating the gradient update evaluated at the sampled point back to a change in the control point. Each client alternates between one epoch of training Θ_i^t and one epoch of training φ . To effectively learn curvature of the loss surface and an orthogonal space of low-loss solutions, as opposed to an effective reparametrisation of the straight line, we enforce that (the dominant component of) $M - \varphi$ lies in the orthogonal complement $\Delta_\theta \mathcal{L}_i(\Theta^t)$, where $M := \frac{1}{2}(\Theta^t + \Theta_i^t)$ is the midpoint of the linear connection. This is achieved by, instead of learning φ directly, learning a control point displacement $\delta\varphi$ which is projected:

$$\varphi = M + (\delta\varphi - \gamma P_{\Delta \mathcal{L}_i(\Theta^t)}(\delta\varphi)) \quad (30)$$

Where $P_{\Delta \mathcal{L}_i(\Theta^t)}$ denotes the orthogonal projection onto $\Delta_\theta \mathcal{L}_i(\Theta^t)$ and $\gamma \in [0, 1]$ is a hyperparameter controlling the strength of the orthogonal complement projection.

Choice of \mathcal{M}_g In keeping with the observations of Section 4, \mathcal{M}_g is chosen as a form of “decaying influence” Bezier surface. In particular, $\hat{\Theta}_i^\tau$ is computed via ORTHODYN described in Section 3 and $\hat{\varphi}_i^\tau$ with the rotational method defined in Equation (17).

\mathcal{M}_g is then defined as the graph of

$$\beta_g^\tau : t \in [0, 1] \mapsto (1-t)^2 \Theta^\tau + t(1-t)\hat{\varphi}_i^\tau + t^2 \hat{\Theta}_i^\tau \quad (31)$$

With $\Theta^{\tau+1} = \beta_g^\tau(\eta_i^\tau)$ where

$$\eta_i^\tau = w_i \eta^\tau \quad (32)$$

For some global learning rate schedule η^τ and global proportion weighting w_i as defined in Equation 1.

The entire server-side procedure is formalised below as Algorithm 1 and the client-side as Algorithm 2. For simplicity, the client-side algorithm is presented with the Adam optimiser.

Algorithm 1: ASYNCCURVE-SERVER

Input: Cyclic learning rate schedule $\eta : \mathbb{N} \rightarrow \mathbb{R}$, initial parameters Θ^0 , number of steps T , SWA proportion σ and cycle length c .

Output: Parameters Θ^{SWA} trained with Stochastic Weight Averaging

Send Θ^0 to each client $k \in [K]$;

$\tau \leftarrow 0$, $\mathbf{n_models} \leftarrow 0$, $\Theta^{\text{SWA}} \leftarrow \Theta^0$;

foreach step $t = 0$ **to** T **do**

if receive $\langle t, \varphi_i^t, \Theta_i^t \rangle$ **then**

 Update estimate of \mathbf{p} ;

$$\hat{\varphi}_i^\tau \leftarrow \frac{\Theta^\tau + \Theta_i^\tau}{2} + R\left(\varphi_i^t - \frac{\Theta^t + \Theta_i^t}{2}\right);$$

$$\hat{\Theta}_i^\tau \leftarrow \text{ORTHODYN}(\Theta_i^t, \Theta^t, \Theta^\tau);$$

$$\alpha \leftarrow \frac{1}{Kp_i} \cdot \eta(\tau);$$

$$\Theta^{\tau+1} \leftarrow (1 - \alpha)^2 \Theta^\tau + \alpha(1 - \alpha) \hat{\varphi}_i^\tau + \alpha^2 \hat{\Theta}_i^\tau;$$

if $\tau \geq \sigma T$ and $\tau \equiv 0 \pmod{c}$ **then**

$$\Theta^{\text{SWA}} \leftarrow \frac{\Theta^{\text{SWA}} \cdot \mathbf{n_models} + \Theta^{\tau+1}}{\mathbf{n_models} + 1};$$

$$\mathbf{n_models} \leftarrow \mathbf{n_models} + 1;$$

end

 Send $\Theta^{\tau+1}$ to client i with initial momentum $\frac{1}{\mathbf{n_batches}_i}(\Theta^\tau - \Theta^{\tau+1})$ and second moment $\frac{1}{\mathbf{n_batches}_i^2}(\Theta^\tau - \Theta^{\tau+1})^{\odot 2}$;

end

$\tau \leftarrow \tau + 1$;

end

return Θ^{SWA}

6 Conclusion

We have surveyed the state-of-the-art in asynchronous delay correction and the applications of geometry to federated learning via mode connectivity. Motivated by this, we introduced the notion of orthogonal DC, in the process uncovering new relationships between loss landscape topography and optimal choice of correction approach, culminating in the novel ORTHODYN algorithm. We generalised previous work to present the ASYNCMANIFOLD algorithmic framework, and proved a convergence result for this class of algorithms that requires only weak assumptions on reasonable component choice. Again inspired by emerging empirical studies, we examined quadratic Bezier curves as a simple instance of a manifold, and devised an efficient rotation-based correction which demonstrates that high-quality low-loss curves can be learned in the AsyncFL setting, showing that they satisfy the manifold quality requirements for ASYNCMANIFOLD. This enabled us to present the novel ASYNCCURVE algorithm for federated optimisation as a proof-of-concept for the framework, the real-world efficacy of which we will examine thoroughly in future experimental work on both canonical deep learning and healthcare-specific datasets.

References

Durmus Alp Emre Acar, Yue Zhao, Ramon Matas Navarro, Matthew Mattina, Paul N. Whatmough, and Venkatesh Saligrama. Federated learning based on dynamic regularization, 2021. URL <https://arxiv.org/abs/2106.02861>.

Algorithm 2: ASYNCCURVE-CLIENT

Data: A global model Θ^t , local endpoint and control point LRs (η_1, η_2) resp., Adam parameters (β_1, β_2) , orthogonality parameter γ , local dataset \mathcal{D}_k , number of epochs E , initial momentum and second moment (v_1, m_1) , and epsilon offset ϵ .

Result: Update triple $\langle t, \varphi_k^t, \Theta_k^t \rangle$

$\theta \leftarrow \Theta^t$;

$c_1 \leftarrow 0, \delta\varphi \leftarrow 0$;

foreach epoch $e = 0$ **to** E **do**

foreach batch \mathcal{B} in \mathcal{D}_k **do**

$c_1 \leftarrow c_1 + 1$;

 Find $g_{\mathcal{B}} \leftarrow \nabla_{\theta} F_i(\mathcal{B}; \theta, \Theta^t)$;

$m_1 \leftarrow \beta_1 m_1 + (1 - \beta_1) g_{\mathcal{B}}$;

$v_1 \leftarrow \beta_2 v_1 + (1 - \beta_2)(g_{\mathcal{B}} \odot g_{\mathcal{B}})$;

$\hat{m} \leftarrow \frac{m_1}{1 - \beta_1^{c_1}}, \hat{v} \leftarrow \frac{v_1}{1 - \beta_2^{c_1}}$;

 Update $\theta \leftarrow \theta - \eta_1 \frac{\hat{m}}{\sqrt{\hat{v} + \epsilon}}$

end

$c_2 \leftarrow 0, m_2 \leftarrow 0, v_2 \leftarrow 0$;

$M \leftarrow \frac{1}{2}(\Theta^t + \theta)$;

foreach batch \mathcal{B} in \mathcal{D}_k **do**

$c_2 \leftarrow c_2 + 1$;

 Sample $\lambda \sim \mathcal{U}[0, 1]$;

 Compute $\varphi \leftarrow M + (\delta\varphi - \gamma P_{\Delta\mathcal{L}_i(\Theta^t)} \delta\varphi)$;

 Compute $\theta_{\lambda} \leftarrow (1 - \lambda)^2 \Theta^t + \lambda(1 - \lambda)\varphi + \lambda^2 \theta$;

 Find $g_{\mathcal{B}} \leftarrow \nabla_{\delta\varphi} \mathcal{L}_i(\mathcal{B}; \theta_{\lambda})$;

$m_2 \leftarrow \beta_1 m_2 + (1 - \beta_1) g_{\mathcal{B}}$;

$v_2 \leftarrow \beta_2 v_2 + (1 - \beta_2)(g_{\mathcal{B}} \odot g_{\mathcal{B}})$;

$\hat{m} \leftarrow \frac{m_2}{1 - \beta_1^{c_2}}, \hat{v} \leftarrow \frac{v_2}{1 - \beta_2^{c_2}}$;

 Update $\delta\varphi \leftarrow \delta\varphi - \eta_2 \frac{\hat{m}}{\sqrt{\hat{v} + \epsilon}}$

end

end

return $\langle t, M + \delta\varphi, \theta \rangle$

[org/abs/2111.04263](https://arxiv.org/abs/2111.04263).

Xuming An, Li Shen, Han Hu, and Yong Luo. Federated learning with manifold regularization and normalized update reaggregation, 2023. URL <https://arxiv.org/abs/2311.05924>.

Gregory W. Benton, Wesley J. Maddox, Sanae Lotfi, and Andrew Gordon Wilson. Loss surface simplexes for mode connecting volumes and fast ensembling, 2021. URL <https://arxiv.org/abs/2102.13042>.

Daniel J. Beutel, Taner Topal, Akhil Mathur, Xinchu Qiu, Javier Fernandez-Marques, Yan Gao, Lorenzo Sani, Kwing Hei Li, Titouan Parcollet, Pedro Porto Buarque de Gusmão, and Nicholas D. Lane. Flower: A friendly federated learning research framework, 2022. URL <https://arxiv.org/abs/2007.14390>.

Silvère Bonnabel. Stochastic gradient descent on riemannian manifolds. *IEEE Transactions on Automatic Control*, 58(9):2217–2229, September 2013. ISSN 1558-2523. doi: 10.1109/tac.2013.2254619. URL <http://dx.doi.org/10.1109/TAC.2013.2254619>.

Debora Caldarola, Barbara Caputo, and Marco Ciccone. Improving generalization in federated learning by seeking flat minima, 2022. URL <https://arxiv.org/abs/2203.11834>.

Sebastian Caldas, Sai Meher Karthik Duddu, Peter Wu, Tian Li, Jakub Konečný, H. Brendan McMahan, Virginia Smith, and Ameet Talwalkar. Leaf: A benchmark for federated settings, 2019. URL <https://arxiv.org/abs/1812.01097>.

-
- Jeffrey Dean, Greg S. Corrado, Rajat Monga, Kai Chen, Matthieu Devin, Quoc V. Le, Mark Z. Mao, Marc’Aurelio Ranzato, Andrew Senior, Paul Tucker, Ke Yang, and Andrew Y. Ng. Large scale distributed deep networks. In *Proceedings of the 26th International Conference on Neural Information Processing Systems - Volume 1*, NIPS’12, pp. 1223–1231, Red Hook, NY, USA, 2012. Curran Associates Inc.
- Pierre Foret, Ariel Kleiner, Hossein Mobahi, and Behnam Neyshabur. Sharpness-aware minimization for efficiently improving generalization, 2021. URL <https://arxiv.org/abs/2010.01412>.
- Timur Garipov, Pavel Izmailov, Dmitrii Podoprikin, Dmitry Vetrov, and Andrew Gordon Wilson. Loss surfaces, mode connectivity, and fast ensembling of dnns, 2018. URL <https://arxiv.org/abs/1802.10026>.
- Dennis Grinwald, Philipp Wiesner, and Shinichi Nakajima. Federated learning over connected modes, 2025. URL <https://arxiv.org/abs/2403.03333>.
- Hao Guo, Jiyong Jin, and Bin Liu. Stochastic weight averaging revisited, 2022. URL <https://arxiv.org/abs/2201.00519>.
- Maxime Haddouche, Paul Viallard, Umut Simsekli, and Benjamin Guedj. A pac-bayesian link between generalisation and flat minima, 2025. URL <https://arxiv.org/abs/2402.08508>.
- Pavel Izmailov, Dmitrii Podoprikin, Timur Garipov, Dmitry Vetrov, and Andrew Gordon Wilson. Averaging weights leads to wider optima and better generalization, 2019. URL <https://arxiv.org/abs/1803.05407>.
- Sai Praneeth Karimireddy, Satyen Kale, Mehryar Mohri, Sashank J. Reddi, Sebastian U. Stich, and Ananda Theertha Suresh. Scaffold: Stochastic controlled averaging for federated learning, 2021. URL <https://arxiv.org/abs/1910.06378>.
- Diederik P. Kingma and Jimmy Ba. Adam: A method for stochastic optimization, 2017. URL <https://arxiv.org/abs/1412.6980>.
- Jungmin Kwon, Jeongseop Kim, Hyunseo Park, and In Kwon Choi. Asam: Adaptive sharpness-aware minimization for scale-invariant learning of deep neural networks, 2021. URL <https://arxiv.org/abs/2102.11600>.
- Marc Law, Renjie Liao, Jake Snell, and Richard Zemel. Lorentzian distance learning for hyperbolic representations. In Kamalika Chaudhuri and Ruslan Salakhutdinov (eds.), *Proceedings of the 36th International Conference on Machine Learning*, volume 97 of *Proceedings of Machine Learning Research*, pp. 3672–3681. PMLR, 09–15 Jun 2019. URL <https://proceedings.mlr.press/v97/law19a.html>.
- Louis Leconte, Matthieu Jonckheere, Sergey Samsonov, and Eric Moulines. Queuing dynamics of asynchronous federated learning, 2024. URL <https://arxiv.org/abs/2405.00017>.
- Y. Lecun, L. Bottou, Y. Bengio, and P. Haffner. Gradient-based learning applied to document recognition. *Proceedings of the IEEE*, 86(11):2278–2324, 1998. doi: 10.1109/5.726791.
- John M Lee. *Riemannian manifolds: an introduction to curvature*, volume 176. Springer Science & Business Media, 2006.
- Hao Li, Zheng Xu, Gavin Taylor, Christoph Studer, and Tom Goldstein. Visualizing the loss landscape of neural nets, 2018. URL <https://arxiv.org/abs/1712.09913>.
- Tian Li, Anit Kumar Sahu, Manzil Zaheer, Maziar Sanjabi, Ameet Talwalkar, and Virginia Smith. Federated optimization in heterogeneous networks, 2020. URL <https://arxiv.org/abs/1812.06127>.
- Ekdeep Singh Lubana, Eric J. Bigelow, Robert P. Dick, David Krueger, and Hidenori Tanaka. Mechanistic mode connectivity, 2023. URL <https://arxiv.org/abs/2211.08422>.

-
- H. Brendan McMahan, Eider Moore, Daniel Ramage, Seth Hampson, and Blaise Agüera y Arcas. Communication-efficient learning of deep networks from decentralized data, 2023. URL <https://arxiv.org/abs/1602.05629>.
- Soheila Molaei, Anshul Thakur, Ghazaleh Niknam, Andrew Soltan, Hadi Zare, and David A Clifton. Federated learning for heterogeneous electronic health records utilising augmented temporal graph attention networks. In Sanjoy Dasgupta, Stephan Mandt, and Yingzhen Li (eds.), *Proceedings of The 27th International Conference on Artificial Intelligence and Statistics*, volume 238 of *Proceedings of Machine Learning Research*, pp. 1342–1350. PMLR, 02–04 May 2024. URL <https://proceedings.mlr.press/v238/molaei24a.html>.
- M. G. Monera, A. Montesinos-Amilibia, and E. Sanabria-Codesal. The taylor expansion of the exponential map and geometric applications, 2012. URL <https://arxiv.org/abs/1210.5971>.
- Maximilian Nickel and Douwe Kiela. Learning continuous hierarchies in the lorentz model of hyperbolic geometry, 2018. URL <https://arxiv.org/abs/1806.03417>.
- Kilian Pfeiffer, Martin Rapp, Ramin Khalili, and Jörg Henkel. Federated learning for computationally constrained heterogeneous devices: A survey. *ACM Computing Surveys*, 55(14s):1–27, July 2023. ISSN 1557-7341. doi: 10.1145/3596907. URL <http://dx.doi.org/10.1145/3596907>.
- Sashank Reddi, Zachary Charles, Manzil Zaheer, Zachary Garrett, Keith Rush, Jakub Konečný, Sanjiv Kumar, and H. Brendan McMahan. Adaptive federated optimization, 2021. URL <https://arxiv.org/abs/2003.00295>.
- Nicola Rieke, Jonny Hancox, Wenqi Li, Fausto Milletari, Holger R. Roth, Shadi Albarqouni, Spyridon Bakas, Mathieu N. Galtier, Bennett A. Landman, Klaus Maier-Hein, Sébastien Ourselin, Micah Sheller, Ronald M. Summers, Andrew Trask, Daguang Xu, Maximilian Baust, and M. Jorge Cardoso. The future of digital health with federated learning. *npj Digital Medicine*, 3(1), September 2020. ISSN 2398-6352. doi: 10.1038/s41746-020-00323-1. URL <http://dx.doi.org/10.1038/s41746-020-00323-1>.
- Chang-Wei Shi, Yi-Rui Yang, and Wu-Jun Li. Ordered momentum for asynchronous sgd, 2025. URL <https://arxiv.org/abs/2407.19234>.
- Andrew A. S. Soltan, Anshul Thakur, Jenny Yang, Anoop Chauhan, Leon G. D’Cruz, Phillip Dickson, Marina A. Soltan, David R. Thickett, David W. Eyre, Tingting Zhu, and David A. Clifton. Scalable federated learning for emergency care using low cost microcomputing: Real-world, privacy preserving development and evaluation of a covid-19 screening test in uk hospitals. *medRxiv*, 2023. doi: 10.1101/2023.05.05.23289554. URL <https://www.medrxiv.org/content/early/2023/05/11/2023.05.05.23289554>.
- Yan Sun, Li Shen, Shixiang Chen, Liang Ding, and Dacheng Tao. Dynamic regularized sharpness aware minimization in federated learning: Approaching global consistency and smooth landscape, 2024. URL <https://arxiv.org/abs/2305.11584>.
- N. Joseph Tatro, Pin-Yu Chen, Payel Das, Igor Melnyk, Prasanna Sattigeri, and Rongjie Lai. Optimizing mode connectivity via neuron alignment, 2020. URL <https://arxiv.org/abs/2009.02439>.
- Hongyi Wang, Mikhail Yurochkin, Yuekai Sun, Dimitris Papailiopoulos, and Yasaman Khazaeni. Federated learning with matched averaging, 2020a. URL <https://arxiv.org/abs/2002.06440>.
- Jianyu Wang, Qinghua Liu, Hao Liang, Gauri Joshi, and H. Vincent Poor. Tackling the objective inconsistency problem in heterogeneous federated optimization, 2020b. URL <https://arxiv.org/abs/2007.07481>.
- Cong Xie, Sanmi Koyejo, and Indranil Gupta. Asynchronous federated optimization, 2020. URL <https://arxiv.org/abs/1903.03934>.
- Chenhao Xu, Youyang Qu, Yong Xiang, and Longxiang Gao. Asynchronous federated learning on heterogeneous devices: A survey, 2023. URL <https://arxiv.org/abs/2109.04269>.

Zhewei Yao, Amir Gholami, Sheng Shen, Mustafa Mustafa, Kurt Keutzer, and Michael W. Mahoney. Adahessian: An adaptive second order optimizer for machine learning, 2021. URL <https://arxiv.org/abs/2006.00719>.

Mang Ye, Xiuwen Fang, Bo Du, Pong C. Yuen, and Dacheng Tao. Heterogeneous federated learning: State-of-the-art and research challenges, 2023. URL <https://arxiv.org/abs/2307.10616>.

Tianhe Yu, Saurabh Kumar, Abhishek Gupta, Sergey Levine, Karol Hausman, and Chelsea Finn. Gradient surgery for multi-task learning, 2020. URL <https://arxiv.org/abs/2001.06782>.

Chen Zhang, Yu Xie, Hang Bai, Bin Yu, Weihong Li, and Yuan Gao. A survey on federated learning. *Knowledge-Based Systems*, 216:106775, 2021. ISSN 0950-7051. doi: <https://doi.org/10.1016/j.knosys.2021.106775>. URL <https://www.sciencedirect.com/science/article/pii/S0950705121000381>.

Shuxin Zheng, Qi Meng, Taifeng Wang, Wei Chen, Nenghai Yu, Zhi-Ming Ma, and Tie-Yan Liu. Asynchronous stochastic gradient descent with delay compensation, 2020. URL <https://arxiv.org/abs/1609.08326>.

Tailin Zhou, Jun Zhang, and Danny H. K. Tsang. Mode connectivity and data heterogeneity of federated learning, 2023. URL <https://arxiv.org/abs/2309.16923>.

A Proofs of Results

Proof of Theorem 1. We begin by bounding $\mathbb{E}[F_{i_s}(\Theta^{s+1}) \mid \Theta^s, i_s]$, which we will abbreviate $\mathbb{E}_s[F_i(\Theta^{s+1})]$. We denote by Δ^s the pseudo-gradient learned for this update, and notice that Assumption 6 gives us an assurance that $\mathbb{E}_s[F(\Theta^{s+1})] \leq \frac{1}{Q} \mathbb{E}_s[F(\Theta^s - \eta_g \Delta^t)]$ for some global learning rate η_g . Accordingly, we will proceed to bound the expected loss at the (linearly interpolated) $\hat{\Theta}^{s+1} := \Theta^s - \eta_g \Delta^t$. Applying Assumption 1 via the descent lemma (we write $i = i_s$ for brevity as it is unambiguous):

$$Q\mathbb{E}_s[\mathcal{L}(\Theta^{s+1})] \leq \mathbb{E}_s[\mathcal{L}(\hat{\Theta}^{s+1})] \leq \mathcal{L}(\Theta^s) + \underbrace{\eta_g \langle \nabla \mathcal{L}(\Theta^s), \mathbb{E}_s[-\Delta^s] \rangle}_{T_1} + \frac{\eta_g^2 L_F}{2} \|\Delta^s\|^2 \quad (33)$$

Assume that $\eta_l < 1$ and $\eta_l = \mathcal{O}(\frac{1}{T-p})$ for some $p > 0$. We begin by bounding T_1 with a manifold curvature term T_Γ that will be expanded later:

$$T_1 \leq T_1 = \langle \nabla \mathcal{L}(\Theta^s), \mathbb{E}_s[-\Delta^s] \rangle \quad (34)$$

$$= \langle \nabla \mathcal{L}(\Theta^s), \mathbb{E}_s[-\Delta^s] + \eta_l K \nabla \mathcal{L}(\Theta^s) - \eta_l K \nabla \mathcal{L}(\Theta^s) \rangle \quad (35)$$

$$= \langle \nabla \mathcal{L}(\Theta^s), \mathbb{E}_s[-\Delta^s] + \eta_l K \nabla \mathcal{L}(\Theta^s) \rangle - \eta_l K \|\nabla \mathcal{L}(\Theta^s)\|^2 \quad (36)$$

$$= \left\langle \nabla \mathcal{L}(\Theta^s), \eta_l K \nabla \mathcal{L}(\Theta^s) + \mathbb{E}_s \left[\sum_{k=0}^{K-1} \Gamma_k - \eta_l \nabla \mathcal{L}(\Theta_{i,k}^t) - \frac{\mu}{2} \eta_l \nabla \|\Theta_{i,k}^t - \Theta^t\|_{\mathcal{M}_0}^2 \right] \right\rangle - \eta_l K \|\nabla \mathcal{L}(\Theta^s)\|^2 \quad (37)$$

$$= \eta_l \left\langle \nabla \mathcal{L}(\Theta^s), \mathbb{E}_s \left[\sum_{k=0}^{K-1} \frac{\Gamma_k}{\eta_l} + \nabla \mathcal{L}(\Theta^s) - \nabla \mathcal{L}(\Theta_{i,k}^t) - \frac{\mu}{2} \nabla \|\Theta_{i,k}^t - \Theta^t\|_{\mathcal{M}_0}^2 \right] \right\rangle - \eta_l K \|\nabla \mathcal{L}(\Theta^s)\|^2 \quad (38)$$

$$= \eta_l \left\langle \sqrt{K} \nabla \mathcal{L}(\Theta^s), \frac{1}{\sqrt{K}} \mathbb{E}_s \left[\sum_{k=0}^{K-1} \frac{\Gamma_k}{\eta_l} + \nabla \mathcal{L}(\Theta^s) - \nabla \mathcal{L}(\Theta_{i,k}^t) - \frac{\mu}{2} \nabla \|\Theta_{i,k}^t - \Theta^t\|_{\mathcal{M}_0}^2 \right] \right\rangle - \eta_l K \|\nabla \mathcal{L}(\Theta^s)\|^2 \quad (39)$$

$$\leq \frac{K\eta_l}{2} \|\nabla \mathcal{L}(\Theta^s)\|^2 + \frac{\eta_l}{2K} \mathbb{E}_s \left\| \sum_{k=0}^{K-1} \frac{\Gamma_k}{\eta_l} + \nabla \mathcal{L}(\Theta^s) - \nabla \mathcal{L}(\Theta_{i,k}^t) - \frac{\mu}{2} \nabla \|\Theta_{i,k}^t - \Theta^t\|_{\mathcal{M}_0}^2 \right\|^2 - \eta_l K \|\nabla \mathcal{L}(\Theta^s)\|^2 \quad (40)$$

$$\leq -\frac{K\eta_l}{2} \|\nabla \mathcal{L}(\Theta^s)\|^2 + \underbrace{\eta_l \mathbb{E}_s \sum_{k=0}^{K-1} \left\| \nabla \mathcal{L}(\Theta^s) - \nabla \mathcal{L}(\Theta_{i,k}^t) - \frac{\mu}{2} \nabla \|\Theta_{i,k}^t - \Theta^t\|_{\mathcal{M}_0}^2 \right\|^2}_{T_2} \quad (41)$$

$$+ \underbrace{\frac{\eta_l}{\eta_l^2} \mathbb{E}_s \sum_{k=0}^{K-1} \|\Gamma_k\|^2}_{T_\Gamma}$$

To expand Δ^s in Equation (37), we have used the property that, under Assumption 5 and by definition, for all Θ :

$$\mathbb{E}_{i \sim \mathbf{P}} \left[\frac{1}{N p_i} \nabla \mathcal{L}_i(\Theta) \right] = \nabla \mathbb{E}_{i \sim \mathbf{P}} \left[\frac{\mathcal{L}_i(\Theta)}{N p_i} \right] = \nabla \mathbb{E}_{i \sim \mathcal{U}} [\mathcal{L}_i(\Theta)] = \nabla \mathcal{L}(\Theta) \quad (42)$$

and in turn the unbiased estimator property of client gradients. We abuse notation and write p_i to denote the estimated probability, where this is the conditional $\mathbf{P}(i \mid \text{time since last update from } i)$. Inequality (40) is given by a simple application of the Cauchy-Schwarz and AM-GM inequalities, along with Jensen's inequality to exchange expectation and norm. (41) is given by the fact that $\|a_1 + \dots + a_K\|^2 \leq K[\|a_1\|^2 + \dots + \|a_K\|^2]$. Substituting back into (33) and rearranging:

$$\frac{K}{2} \|\nabla \mathcal{L}(\Theta^s)\|^2 \leq T_2 + \frac{1}{\eta_l^2} T_\Gamma + \left(\frac{\mathcal{L}(\Theta^s) - Q \mathbb{E}_s[\mathcal{L}(\Theta^{s+1})]}{\eta_g \eta_l} \right) + \frac{\eta_g L_F}{2\eta_l} \|\Delta^s\|^2 \quad (43)$$

The manifold curvature terms Γ_k quantify the difference between a step along the unique geodesic in the ambient manifold with initial tangent vector $\nabla F_i(\Theta_{i,k}^t)$ and the initial tangent vector. Notice that where the manifold is totally geodesic (in particular, where the ambient manifold is Euclidean), the tangent is constant along the line, so $T_\Gamma = 0$. We bound it via Assumption 8 in the arbitrary case. Let $\bar{\nabla}$ denote the normalised

gradient, then:

$$T_{\Gamma} \leq \mathbb{E}_s \sum_{k=0}^{K-1} \left\| -\eta_l \nabla F_i(\Theta_{i,k}^t) - (\Theta_{i,k}^t - \exp_{\Theta_{i,k}^t}(\eta_l \nabla F_i(\Theta_{i,k}^t))) \right\|^2 \quad (44)$$

$$\begin{aligned} &\leq \mathbb{E}_s \sum_{k=0}^{K-1} \left\| -\eta_l \nabla F_i(\Theta_{i,k}^t) - (\Theta_{i,k}^t - \Theta_{i,k}^t - \eta_l \|\nabla F_i(\Theta_{i,k}^t)\| \bar{\nabla} F_i(\Theta_{i,k}^t) \right. \\ &\quad \left. - \frac{1}{2} \eta_l^2 \|\nabla F_i(\Theta_{i,k}^t)\|^2 \gamma_{\bar{\nabla} F_i(\Theta_{i,k}^t)}''(0) - \mathcal{O}(C \eta_l^3 \|\nabla F_i(\Theta_{i,k}^t)\|^3) \right\|^2 \end{aligned} \quad (45)$$

$$\leq \mathbb{E}_s \sum_{k=0}^{K-1} \left\| \frac{1}{2} \eta_l^2 \|\nabla F_i(\Theta_{i,k}^t)\|^2 \gamma_{\bar{\nabla} F_i(\Theta_{i,k}^t)}''(0) + \mathcal{O}(C \eta_l^3 \|\nabla F_i(\Theta_{i,k}^t)\|^3) \right\|^2 \quad (46)$$

$$= \mathbb{E}_s \sum_{k=0}^{K-1} \mathcal{O} \left\| \eta_l^2 \|\nabla F_i(\Theta_{i,k}^t)\|^2 \gamma_{\bar{\nabla} F_i(\Theta_{i,k}^t)}''(0) \right\|^2 + \mathcal{O} \|C \eta_l^3 \|\nabla F_i(\Theta_{i,k}^t)\|^3\|^2 \quad (47)$$

$$= \mathbb{E}_s \sum_{k=0}^{K-1} \mathcal{O} (\eta_l^4 G_2^4 \cdot C^2) + \mathcal{O} (\eta_l^6 G_2^6 \cdot C^2) \quad (48)$$

$$\leq \mathcal{O} \left(K \eta_l^4 \cdot \underbrace{G_2^4 C^2 (1 + \eta_l^2 G_2^2)}_{A_{\Gamma}} \right) \quad (49)$$

Where (45) is given by considering the Taylor expansion of the exponential map around $\Theta_{i,k}^t$, on the assumption that - following the same technique as [Bonnabel \(2013\)](#) - T is large enough that $\|\eta_l \nabla F_i(\Theta_{i,k}^t)\| < I$. We note that the cubic error term with η_l factored out is known to be bounded (dependent on the curvature bound C) via the Gauss-Codazzi equations, but we omit a detailed exploration of the exact dependence of the convergence rate on manifold curvature. See [Monera et al. \(2012\)](#) for a more thorough treatment of this Taylor expansion.

Aside. We briefly consider the properties of the proximal term $\frac{\mu}{2} \nabla \|\Theta_{i,k}^t - \Theta^t\|_{\mathcal{M}_0}^2$ (a shorthand for projecting into \mathcal{M}_0 and then taking the norm). Applying the chain rule:

$$\frac{\mu}{2} \nabla \|\pi_{\mathcal{M}_0}(\Theta_{i,k}^t) - \pi_{\mathcal{M}_0}(\Theta^t)\|_{\mathcal{M}_0}^2 = \mu \cdot \mathcal{J}_{\Theta}(\pi)|_{\Theta_{i,k}^t} \cdot (\pi(\Theta_{i,k}^t) - \pi(\Theta^t)) \quad (50)$$

Here, the simple form of the derivative of the norm comes from the assumption that π projects onto the coordinate system of an orthonormal basis for \mathcal{M}_0 , hence $\|\pi(\Theta)\|_{\mathcal{M}_0} = \sum_{i \in [\dim \mathcal{M}_0]} \pi(\Theta)_i^2$. Where the ambient manifold is equal \mathcal{M}_0 , hence π is the identity, this allows us to telescope the pseudo-gradient sum and arrive at:

$$\mathbb{E}_s [-\Delta^s] = \eta_l \sum_{k=0}^{K-1} -\nabla \mathcal{L}(\Theta_{i,k}^t) - \mu (\Theta_{i,k}^t - \Theta^t) \quad (51)$$

$$= \eta_l \sum_{k=0}^{K-1} -\nabla \mathcal{L}(\Theta_{i,k}^t) (1 - \mu)^{K-1-k} \quad (52)$$

In general, this will encourage the drift $\mathbb{E} \|\Theta^t - \Theta_{i,k}^t\|$ to be smaller, and hence by smoothness the difference in the bound on the gradient norms of \mathcal{L} at each point to be reduced. However, our analysis will allow divergence between the norms in \mathcal{M}_0 and the ambient manifold, leading to an increase proximal weight μ counter-intuitively increasing the final rate of convergence we derive. The reason for this is philosophical: where \mathcal{M}_0 is the ambient manifold, the proximal term acts purely as regularisation, discouraging movement away from the global mode. If the norm on \mathcal{M}_0 is chosen to more accurately capture the loss landscape, and the local step occurs in an area of high divergence, then this term can actually encourage movement away from the global mode relative to the ambient norm (the reference norm for the convergence result).

Turning our attention to bounding T_2 :

$$T_2 \leq \sum_{k=0}^{K-1} 2\mathbb{E}_s \left\| \nabla \mathcal{L}(\Theta^s) - \nabla \mathcal{L}(\Theta_{i,k}^t) \right\|^2 + \frac{\mu^2}{2} \mathbb{E}_s \left\| \nabla \left\| \Theta_{i,k}^t - \Theta^t \right\|_{\mathcal{M}_0}^2 \right\|^2 \quad (53)$$

$$\leq \sum_{k=0}^{K-1} 2L_F^2 \mathbb{E}_s \left\| \Theta^s - \Theta_{i,k}^t \right\|^2 + \frac{\mu^2}{2} L_N^2 \mathbb{E}_s \left\| \Theta^t - \Theta_{i,k}^t \right\|^2 \quad (54)$$

$$\leq \sum_{k=0}^{K-1} 4L_F^2 \left(\mathbb{E}_s \left\| \Theta^s - \Theta^t \right\|^2 + \mathbb{E}_s \left\| \Theta^t - \Theta_{i,k}^t \right\|^2 \right) + \frac{\mu^2}{2} L_N^2 \mathbb{E}_s \left\| \Theta^t - \Theta_{i,k}^t \right\|^2 \quad (55)$$

Aside. Notice that, when separating terms in Equation (54), the proof can be trivially modified at this stage to change the pseudo-gradient to the trusted position form of delay correction by adding an extra drift term. Whilst beyond the scope of the current work, we also see how it would be possible to account for delay correction more generally by bounding the difference between the received pseudo-gradient (evaluated at Θ^t) and the pseudo-gradient evaluated at Θ^s , as a quality multiplier on the difference when the pseudo-gradient is unmodified.

Naturally, we now bound the local drift:

$$\mathbb{E}_s \left\| \Theta_{i,k}^t - \Theta^t \right\|^2 \leq \left(1 + \frac{1}{K-1} \right) \mathbb{E}_s \left\| \Theta_{i,k-1}^t - \Theta^t \right\|^2 + K \mathbb{E}_s \left\| -\eta_l g_{i,k-1}^t \right\|^2 \quad (56)$$

This equation is trivial when the ambient manifold is Euclidean, but requires a little justification where the local steps are along non-Euclidean (distance minimising, arc-length parametrised) geodesics. Recall that the learning rate η_l defines the distance along the geodesic γ with initial tangent $g_{i,k-1}^t$, proportional to the movement of the exponential map. Under arc-length parametrisation, this means that each step moves the local mode to $\gamma(\eta_l \|g_{i,k-1}^t\|)$. Since the geodesic is distance-minimizing, we have that $\|\Theta_{i,k}^t - \Theta_{i,k-1}^t\| = \eta_l \|g_{i,k-1}^t\|$, as required to separate the norms. Continuing:

$$\begin{aligned} \mathbb{E}_s \left\| \Theta_{i,k}^t - \Theta^t \right\|^2 &\leq \left(1 + \frac{1}{K-1} \right) \mathbb{E}_s \left\| \Theta_{i,k-1}^t - \Theta^t \right\|^2 + K \eta_l^2 \mathbb{E}_s \left\| g_{i,k-1}^t - \nabla \mathcal{L}_i(\Theta_{i,k-1}^t) + \nabla \mathcal{L}_i(\Theta_{i,k-1}^t) \right\|^2 \\ &\quad - \frac{\mu}{2} \nabla \left\| \Theta_{i,k-1}^t - \Theta^t \right\|_{\mathcal{M}_0}^2 + \frac{\mu}{2} \nabla \left\| \Theta_{i,k-1}^t - \Theta^t \right\|_{\mathcal{M}_0}^2 \end{aligned} \quad (57)$$

$$\leq \left(1 + \frac{1}{K-1} \right) \mathbb{E}_s \left\| \Theta_{i,k-1}^t - \Theta^t \right\|^2 + K \eta_l^2 \sigma_l^2 + \quad (58)$$

$$+ 2K \eta_l^2 \mathbb{E}_s \left\| \nabla \mathcal{L}_i(\Theta_{i,k-1}^t) + \frac{\mu}{2} \nabla \left\| \Theta_{i,k-1}^t - \Theta^t \right\|_{\mathcal{M}_0}^2 \right\|^2$$

$$\leq \left(1 + \frac{1}{K-1} \right) \mathbb{E}_s \left\| \Theta_{i,k-1}^t - \Theta^t \right\|^2 + 4K \eta_l^2 G^2 + K \eta_l^2 \sigma_l^2 + K \eta_l^2 \mu^2 L_N^2 \mathbb{E}_s \left\| \Theta_{i,k-1}^t - \Theta^t \right\|^2 \quad (59)$$

$$= \left(1 + \frac{1}{K-1} + K \eta_l^2 \mu^2 L_N^2 \right) \mathbb{E}_s \left\| \Theta_{i,k-1}^t - \Theta^t \right\|^2 + 4K \eta_l^2 G^2 + K \eta_l^2 \sigma_l^2 \quad (60)$$

Where we have used the unbiased estimator property of $g_{i,k-1}^t$ in Equation (58) and Equation (59) follows immediately from Assumptions 1 and 3. Suppose now that $\mu > 0$ and $\eta_l < \frac{1}{\mu L_N K}$. We unroll this recursive bound to find:

$$\mathbb{E}_s \left\| \Theta_{i,k}^t - \Theta^t \right\|^2 \leq \sum_{p=0}^{k-1} \left(1 + \frac{1}{K-1} \right)^p \cdot (4K \eta_l^2 G^2 + K \eta_l^2 \sigma_l^2) \quad (61)$$

$$\leq (4K \eta_l^2 G^2 + K \eta_l^2 \sigma_l^2) \cdot (K-1) \cdot \left(\left(1 + \frac{1}{K-1} \right)^K - 1 \right) \quad (62)$$

$$\leq 5K^2 \eta_l^2 (4G^2 + \sigma_l^2) \quad (63)$$

Note that this would become still hold when $\mu = 0$, we simply do not require any restriction on η_l . Equation (63) uses the fact that $(1 + \frac{1}{K-1})^K \leq 5$ for $K > 1$ (Reddi et al., 2021).

Now note that Assumptions 4 and 7 bound the global drift $\|\Theta^s - \Theta^t\|$ in terms of the bound on the local drift $\|\Theta^t - \Theta_{i,K}^t\|$. In particular:

$$\mathbb{E}_{t,\dots,s} \|\Theta^s - \Theta^t\|^2 \leq S^2 D^2 \eta_g^2 \mathbb{E}_{t^{worst}} \left\| \Theta_{i,K}^{t^{worst}} - \Theta^{t^{worst}} \right\|^2 \leq 5 S^2 D^2 \eta_g^2 K^2 \eta_l^2 (4G^2 + \sigma_l^2) \quad (64)$$

We can now pick up where we left off at Equation (55):

$$T_2 \leq \sum_{k=0}^{K-1} 4L_F^2 \left(\mathbb{E}_s \|\Theta^s - \Theta^t\|^2 + \mathbb{E}_s \|\Theta^t - \Theta_{i,k}^t\|^2 \right) + \frac{\mu^2}{2} L_N^2 \mathbb{E}_s \|\Theta^t - \Theta_{i,k}^t\|^2 \quad (65)$$

$$\leq \sum_{k=0}^{K-1} 20L_F^2 K^2 \eta_l^2 (4G^2 + \sigma_l^2) (1 + S^2 D^2 \eta_g^2) + 10\mu^2 L_N^2 K^2 \eta_l^2 G^2 \quad (66)$$

$$= \mathcal{O} \left(K^3 \eta_l^2 \cdot \underbrace{(L_F^2 (1 + S^2 D^2 \eta_g^2) (4G^2 + \sigma_l^2) + \mu^2 L_N^2 G^2)}_{A_D} \right) \quad (67)$$

We can now substitute the bounds on T_2 in Equation (67), T_Γ in (49), and the local drift in (63) into Equation (43):

$$\|\nabla \mathcal{L}(\Theta^s)\|^2 \leq \mathcal{O}(K^2 \eta_l^2 \cdot A_D) + \mathcal{O}(\eta_l^2 \cdot A_\Gamma) + \left(\frac{\mathcal{L}(\Theta^s) - Q \mathbb{E}_s[\mathcal{L}(\Theta^{s+1})]}{K \eta_g \eta_l} \right) + 5\eta_g L_F K \eta_l (4G^2 + \sigma_l^2) \quad (68)$$

We now sum over $s \in [0..T-1]$ and rearrange to be in the form of the final result, noticing that the sum of loss terms in (68) telescope. Letting Ψ be as in the statement of the theorem:

$$\mathbb{E} \left[\frac{1}{T} \sum_{s=0}^{T-1} \|\nabla \mathcal{L}(\Theta^s)\|^2 \right] \leq \mathcal{O} \left(\frac{\mathcal{L}(\Theta^0) - \mathcal{L}(\Theta^*)}{TK \eta_g \eta_l} + \frac{\Psi}{K \eta_g \eta_l} \right) + \mathcal{O}(\eta_g L_F K \eta_l (4G^2 + \sigma_l^2)) + \mathcal{O}(\eta_l^2 (K^2 A_D + A_\Gamma)) \quad (69)$$

The result then follows by choosing an appropriate schedule for $\{K, \eta_g, \eta_l\}$.

□